

## In vivo demonstration of amyloid burden in posterior cortical atrophy: a case series with PET and CSF findings

Maité Formaglio · Nicolas Costes · Jérémie Seguin · Yannick Tholance · Didier Le Bars · Isabelle Rouillet-Solignac · Bernadette Mercier · Pierre Krolak-Salmon · Alain Vighetto

Received: 28 July 2010/Revised: 18 January 2011/Accepted: 24 March 2011/Published online: 10 April 2011  
© Springer-Verlag 2011

**Abstract** Our objective was to evaluate amyloid deposition in posterior cortical atrophy (PCA), using both cerebrospinal fluid (CSF) biomarker analysis and amyloid imaging. Five PCA patients, selected based on their neuropsychological profile and atrophic changes in posterior regions on MRI, underwent CSF analysis. CSF amyloid-beta 1–42, total tau, and phosphorylated tau at threonine

181 levels were determined. They also had positron emission tomography (PET) with Pittsburgh Compound B ( $^{11}\text{C}$ PIB).  $^{11}\text{C}$ PIB ratio images were assessed with visual, regional and voxel-based analyses and compared to eight typical Alzheimer's disease (AD) patients and eight controls. The biological profile in the five PCA patients, resulting from CSF and  $^{11}\text{C}$ PIB images analysis, was consistent with AD. Individual comparisons of PCA patients'  $^{11}\text{C}$ PIB images with the AD group with Statistical Parametric Mapping (SPM) revealed a distinctive posterior uptake in four out of the five patients showing increased amyloid deposition in occipital, temporal, and/or parietal regions. ROI group analysis showed a tendency for higher amyloid deposition in occipital and temporal regions. However, this pattern was not found with SPM group analysis when the global level of  $^{11}\text{C}$ PIB uptake was used as a covariate. Our results indicate that amyloid burden can be demonstrated in vivo in PCA suggesting a diagnosis of AD. PCA patients may present a higher global amyloid load than AD that was not related to age at onset, disease severity, disease duration, or educational level in our study. Combined CSF and PET biomarkers seem helpful for in vivo diagnosis of this focal syndrome with underlying AD pathology.

M. Formaglio (✉) · I. Rouillet-Solignac · B. Mercier · P. Krolak-Salmon · A. Vighetto  
Department of Neurology, Service de Neurologie D, Hospices Civils de Lyon, Hôpital Neurologique, 59 boulevard Pinel, 69003 Lyon, France  
e-mail: maite.formaglio@chu-lyon.fr

N. Costes · D. Le Bars  
CERMEP, Imagerie du vivant, 59 boulevard Pinel, 69003 Lyon, France

J. Seguin · Y. Tholance  
Neurobiology Laboratory, Department of Biochemistry, Hospices Civils de Lyon, Centre de Biologie et de Pathologie Est, 59 boulevard Pinel, 69003 Lyon, France

M. Formaglio · N. Costes · J. Seguin · Y. Tholance · D. Le Bars · P. Krolak-Salmon · A. Vighetto  
Lyon 1 University, Lyon, France

P. Krolak-Salmon  
INSERM Unit 821, Cerebral Dynamics and Cognition, Centre Hospitalier le Vinatier, 95 boulevard Pinel, 69500 Bron, France

A. Vighetto  
INSERM UMR-S 864, Space and Action, 16 avenue du Doyen Lépine, 69676 Bron Cedex, France

M. Formaglio · I. Rouillet-Solignac · B. Mercier · P. Krolak-Salmon · A. Vighetto  
Center for Memory Resources and Research, Hospices Civils de Lyon, Lyon, France

**Keywords** Posterior cortical atrophy · Pittsburgh Compound B · PET · Voxel based analysis · CSF biomarkers · Alzheimer's disease

### Introduction

Posterior cortical atrophy (PCA) is a rare neurodegenerative syndrome. It is characterized by progressive development of higher-order visuooperative deficits, in addition to

atrophic or metabolic changes in the posterior regions of the brain [1–4]. Clinical features may include Balint's syndrome, Gerstmann's syndrome, alexia, visual object agnosia, visuospatial neglect, prosopagnosia, environmental disorientation and apraxia. Homonymous hemianopia may also be present [5]. Magnetic resonance imaging (MRI) usually shows cortical atrophy in the parietal, occipital and posterior temporal regions [6], while [ $^{18}\text{F}$ ]fluorodeoxyglucose positron emission tomography (FDG-PET) may reveal hypometabolism in the posterior cerebral hemispheres, even in the absence of concomitant atrophy [7, 8]. This syndrome almost universally progresses to more diffuse cognitive impairment and dementia.

Histologically, PCA is most often associated with Alzheimer's disease (AD) pathology [9]. Neurofibrillary tangles (NFT), corresponding to tau protein deposits, are preferentially located in the posterior cortex, including primary visual cortex and visual associative areas [2, 3]. Senile plaques (SPs), corresponding to amyloid deposits, may also predominate posteriorly but this finding is more controversial [2, 10].

Cerebrospinal fluid (CSF) levels of amyloid-beta 1–42 ( $\text{A}_{42}$ ) are decreased in AD, and those of total tau (T-tau) and tau phosphorylated at threonine 181 (P-tau181) are increased. When levels of all three are combined into a single biomarker, both sensitivity and specificity for diagnosing AD are in the region of 90% [11, 12].

The PET imaging radioligand Pittsburgh Compound B ( $^{11}\text{C}$ PIB) allows in vivo assessment of  $\text{A}\beta$  plaque burden. PIB is a derivative of thioflavin T that binds specifically to fibrillar  $\text{A}\beta$  deposits in human brain [13]. Human PET studies have shown significantly higher neocortical retention of  $^{11}\text{C}$ PIB in AD than controls [14, 15], reflecting the presence of  $\text{A}\beta$  plaques and amyloid angiopathy [16–18].

We studied amyloid deposition in five PCA patients, using CSF biomarker analysis and  $^{11}\text{C}$ PIB imaging with visual, regional and voxel-based analyses. Eight typical AD patients and eight controls also had  $^{11}\text{C}$ PIB imaging for comparison. Our objective was to demonstrate in vivo amyloid burden in PCA and to reveal any specific pattern of cortical deposit in comparison to typical AD.

## Materials and methods

### Subjects

#### PCA subjects

Five PCA patients (mean age:  $65.2 \pm 7.6$  years; MMSE [19]:  $20.4 \pm 5$ ; CDR [20]:  $1 \pm 0$ ; Table 1) were prospectively recruited from our memory clinic. PCA was

diagnosed according to the following diagnostic criteria [Renner et al. (2004), McMonagle et al. (2006)]: (1) History of progressive acquired visual impairment, interfering with daily life, and not due to ophthalmological abnormalities. (2) Evidence of one or several disorders reflecting dysfunction of occipito-parieto-temporal association cortices, such as Balint's syndrome, Gerstmann's syndrome or apraxia. (3) Absent or minor memory impairment, executive dysfunction or language deficits. (4) Evidence of atrophy of the posterior cortex on MRI, or of reduced regional blood flow on [ $^{99}\text{Tc}$ ]HMPAO SPECT. A visual analysis of MRI and, when available, SPECT images was performed for each patient at their inclusion in the study. Patients showing major vascular lesions on MRI were excluded from the study. All PCA patients underwent full ophthalmological testing, including visual field determination. They all underwent a lumbar puncture for CSF biomarkers analysis and amyloid PET imaging with  $^{11}\text{C}$ PIB.

#### AD group

Eight patients (mean age:  $74.6 \pm 6.2$  years; MMSE:  $21.4 \pm 5.9$ , CDR:  $1.2 \pm 0.4$ ) with mild or moderate AD were recruited from our memory clinic as a comparison group for  $^{11}\text{C}$ PIB analysis (Table 2). They had a history of progressive cognitive impairment with mild or moderate weakening of autonomy; memory complaint; and memory impairment at neuropsychological testing. The other cognitive functions could be variably affected. AD patients met the NINCDS-ADRDA diagnostic criteria for probable AD [21]. They underwent the same neuropsychological tests and imaging as PCA patients. Visual analysis of amyloid PET imaging showed increased  $^{11}\text{C}$ PIB binding consistent with probable AD in all.

#### Control group

Eight normal volunteers (mean age:  $73.9 \pm 6.1$  years, MMSE:  $29.4 \pm 0.7$ , CDR: 0) without cognitive complaints were recruited from the community by advertisement as a comparison group for  $^{11}\text{C}$ PIB analysis. All were free of relevant medical illness. Control subjects were screened via an evaluation that included a medical history, functional assessment, neurological examination and neuropsychological testing. Only cognitively intact subjects were included. They all had normal  $^{11}\text{C}$ PIB binding on PET according to visual analysis.

All patients and controls gave their written informed consent to participate. The study was approved by the institutional ethics committee.  $^{11}\text{C}$ PIB PET scanning in humans was approved by the French regulatory authorities (AFSSAPS).

**Table 1** Demographic characteristics and clinical features of PCA patients

Subjects	PCA 1	PCA 2	PCA 3	PCA 4	PCA 5
Age at Imaging (y)	63	65	54	74	70
Education (y)	11	12	10	11	11
Sex (M/F)	F	M	M	M	F
Initial complaint	Driving	Reading	Getting lost writing	Reading Writing Driving	Reading Writing
Duration of symptoms at presentation (y)	2	1–2	1–2	3–4	3
MMSE/30 at PET	28	22	20	15	17
CDR at PET	0.5	0.5	0.5	1.5	1
Full Balint syndrome	x	x	–	x	x
Isolated simultanagnosia	–	–	x	–	–
Full Gerstmann syndrome	–	–	x	–	x
Isolated acalculia	–	x	–	x	x
Isolated agraphia	x	x	–	x	x
Apraxia					
Dressing	–	–	–	x	x
Ideomotor	x	–	x	x	x
Constructional	x	x	x	x	x
Alexia	x	x		x	x
Environmental agnosia	–	–	x	x	x
Visuospatial neglect	x	–	–	–	x
Visual field examination	Visual attention deficit	Left hemianopia	Normal	Visual attention deficit	Left hemianopia
Hallucinations	–	–	–	–	x
Fluctuations	–	–	–	–	–
Mild Parkinsonism	x	–	x	–	–

MMSE Mini-mental state examination, CDR Clinical dementia rating, x clinical signs observed, – clinical signs not observed

**Table 2** Demographic characteristics of AD patients

Subjects	Age at imaging (y)	Education (y)	Gender (M/F)	Duration of symptoms at presentation (y)	MMSE at PET/30	CDR at PET
AD 1	77	8	F	2	24	0.5
AD 2	84	9	F	1	24	1
AD 3	80	13	F	2	26	1
AD 4	66	11	F	3	27	0.5
AD 5	66	9	M	4	7	2
AD 6	70	9	F	4	20	1
AD 7	75	8	M	5	22	1
AD 8	79	9	F	5	21	1

*Statistical analysis*

Demographic and neuropsychological data were compared between PCA and AD groups using a non-parametric test (Mann–Whitney *U*) because of the small sample size; *p* values <0.05 were considered significant (Table 3). Analysis was performed with MedCalc® version 11.1.1.0

(Frank Schoonjans, MedCalc Software, Mariakerke, Belgium).

Neuropsychological evaluation

Verbal episodic memory was assessed with the Free and Cued Selective Recall Reminding Test (FCSRT) [22] or

**Table 3** Neuropsychological data of PCA and AD patients

Subjects	Age (y)	Education (y)	Disease duration (y)	MMSE/30	CDR	FCSRT free recall/48	FCSRT free recall/48	FCSRT free recall/16	FCSRT total delayed recall/16	FCSRT intrusions	FCSRT recognition/16	TMT-A	TMT-B	STROOP (inhibition condition)	Verbal fluency (letter P)	Verbal fluency (animals)	Bachy/36	Figures copying/drawing/7	Clock	VOSP incomplete letters/20	VOSP number location/10	
PCA 1	63	11	2	28	0.5	33	47	12	16	2	16	282	340	NF	15	25	36	1	3	14	NF	
PCA 2	54	12	2	20	0.5	8	25	4	11	10	15	178	NF	20.34	8	18	36	0	0	NF	NF	
PCA 3	74	10	4	15	1	3	8	NF	NF	NF	NF	NF	NF	NF	5	10	31	0	0	NF	NF	
PCA 4	65	11	2	22	0.5	NF	NF	NF	NF	NF	NF	222	NF	NF	14	16	33	0	6	14	5	
PCA 5	70	11	3	17	1	19	42	14	15	10	15	NF	NF	NF	13	12	NF	0	0	NF	NF	
Mean ± SD	65.2 ± 7.6	11 ± 7.6	2.6 ± 0.9	20.4 ± 5.0	1 ± 0	15.75 ± 13.3	30.5 ± 17.7	10 ± 5.3	14 ± 2.6	7.33 ± 4.6	15.3 ± 0.6	227.3 ± 52.2	340	20.34	11 ± 4.3	16.2 ± 5.8	34 ± 2.4	0.2 ± 0.4	1.8 ± 2.7	14	5	
AD 1	77	8	2	24	0.5	2	18	0	7	22	16	42	NR	42.1	14	14	34	1	5	18	NA	
AD 2	84	9	1	24	1	14	32	2	13	6	16	65	180	NA	11	13	30	1	NA	NA	NA	
AD 3	80	13	2	26	1	8	27	1	6	9	15	98	224	33.26	10	14	36	1	5	20	NA	
AD 4	66	11	3	27	0.5	7	33	1	9	40	16	112	262	39.6	17	9	36	3	7	NA	NA	
AD 5	66	9	4	7	2	NF	NF	NF	NF	NF	NF	NF	NF	NA	NF	NF	NF	NF	NF	NF	NF	
AD 6	70	9	4	20	1	2	6	NF	NF	NF	16	129	347	NA	12	10	34	3	4	NA	NA	
AD 7	75	8	5	22	1	2	8	0	2	19	14	67	197	NA	8	21	36	3	NA	20	9	
AD 8	79	9	5	21	1	2	16	2	8	7	16	73	271	30.49	8	11	30	3	4	NA	NF	
Mean ± SD	74.6 ± 6.2	9.5 ± 1.6	3.3 ± 1.4	21.4 ± 5.9	1.2 ± 0.4	5.3 ± 4.3	20 ± 10.2	1 ± 0.8	7.5 ± 3.3	17.17 ± 11.9	15.6 ± 0.7	83.7 ± 28.1	246.8 ± 55.3	36.4 ± 5.4	11.4 ± 3	13.1 ± 3.7	33.7 ± 2.5	2.1 ± 1	5 ± 1.1	19.3 ± 0.9	9	
<i>p</i> -Value	<b>0.03</b>	0.06	0.41	0.46	0.21	0.07	0.3	<b>0.02</b>	<b>0.048</b>	0.44	0.46	<b>0.02</b>	–	–	1	0.33	0.86	<b>0.008</b>	0.08	0.08	–	–

Significant *p* value < 0.05 are highlighted

FCSRT Free and Cued Selective Reminding Test, CVLT California Verbal Learning Test, TMT Trail Making Test, STROOP Stroop test, Bachy Bachy-Langedock denomination task, VOSP Visual object and space perception battery, NF not feasible due to patient's cognitive difficulties, NA not assessed

the French version of the California Verbal Learning Test [23]. We explored verbal fluency [24] and naming with the Bachy-Langedock denomination task [25]. Executive functions were assessed with the Stroop Test [26] or the Trail Making Test [27]. Visuospatial, visuoperceptive and visuoconstructive abilities were assessed with the Visual Object and Space Perception battery [28], the clock drawing test [29], and complex figure copying tests. Praxis were most often evaluated with informal personal procedures. These neuropsychological tests and PIB-PET were performed within the same month, and both within 1 year after the lumbar puncture.

#### CSF data

##### *CSF sampling and storage*

CSF sampling was performed according to a standard protocol. In total, 10 mL were collected in polypropylene vials and then centrifuged immediately. Supernatant was sampled in polypropylene vials and aliquots were stored at  $-80^{\circ}\text{C}$  until analysis.

##### *CSF analysis*

CSF T-tau, P-tau181 and  $A\beta_{42}$  levels were determined using a commercially available ELISA kit (INNOTEST httau-Ag, INNOTEST Phospho-Tau<sub>(181)</sub>, INNOTEST  $\beta$ -amyloid<sub>(1-42)</sub>, respectively, Innogenetics<sup>®</sup>, Gent, Belgium) according to the manufacturer's instructions. All biomarker levels were measured in duplicate. The inter-assay coefficient of variation was less than 10%. Cut-off values were determined from literature data and experience of our neurobiology department, and were T-tau  $>350$  pg/mL, P-tau181  $>60$  pg/mL and  $A\beta_{42}$   $<500$  pg/mL [30–32]. If all three levels lay beyond these cut-off values, subjects were considered to have a typical AD profile. CSF pattern was said atypical for patients with either elevated T-tau  $>350$  pg/mL and P-tau181  $>60$  pg/mL or decreased  $A\beta_{42}$   $<500$  pg/mL.

#### PET imaging

##### *Radiochemistry*

[ $^{11}\text{C}$ ]PIB was produced by methylation of 1.2 mg of its desmethyl precursor 6-OH-BTA-0 (ABX Germany) with [ $^{11}\text{C}$ ]methyl triflate in 200  $\mu\text{L}$  acetone for 3 min at  $100^{\circ}\text{C}$ , with a Bioscan MeI + synthesizer, starting from [ $^{11}\text{C}$ ]O<sub>2</sub> produced via a  $^{14}\text{N}(p,\alpha)^{11}\text{C}$  nuclear reaction using an IBA Cyclone 18/9 cyclotron. The reaction product was purified using high-performance liquid chromatography with a SymetryPrep column (Waters) using water/acetonitrile

(50:50) at 3 mL/min. The collected fraction was loaded on a C18 SepPak, washed with 10 mL of water and eluted with 1 mL absolute ethanol. After addition of NaCl 0.9% the product was sterilized through a 0.22  $\mu\text{m}$  Millipore sterile filter (Waters). The radioligand purity was assessed by analytical radio-HPLC (Beckman 32 K). Radiochemical purity was in excess of 95%, and specific activity in the range of 10–40 GBq/ $\mu\text{mol}$ .

##### *PET imaging*

PET scans were performed on a CTI-Siemens HR + scanner (Knoxville, TN, USA). For tracer injections, an intravenous catheter was placed in a vein of the left forearm. Before emission acquisition, a 10-min transmission scan was performed using three  $^{68}\text{Ge}$  rod sources for the measurement of tissue and head support attenuation. After i.v. injection of a bolus of [ $^{11}\text{C}$ ]PIB ( $470 \pm 12$  MBq), a dynamic emission scan consisting of 34 frames of increasing duration (20 s–5 min) was acquired over 90 min. The PET scanner was operating in 3D mode. Images were corrected for scatter and attenuation, and reconstructed using a filtered back projection (Hanning filter, cut-off 0.5 cycles/pixels) to provide a 3D volume of 63 slices (2.42 mm thickness) with  $128 \times 128$  voxels in plane ( $2.06 \text{ mm}^2$ ).

##### *MRI*

Structural brain MRI was performed using a 1.5 T Siemens Magnetom scanner (Siemens AG, Erlangen, Germany), with a 3D anatomical T1-weighted sequence (TR: 9.7 ms, TE: 4 ms) covering the whole brain volume with  $1 \text{ mm}^3$  cubic voxels.

##### *Visual analysis*

Voxel based [ $^{11}\text{C}$ ]PIB parametric RATIO images were computed by dividing, for each voxel, the integrated activity over the 40–90 min interval by integrated activity of the reference region (cerebellar gray matter) for the same interval. [ $^{11}\text{C}$ ]PIB-RATIO images were read by a neurologist unaware of the clinical diagnosis. Images were graded as normal (similar to controls), doubtful or probable AD. Transverse, sagittal, and coronal views were available for viewing. Before reading the [ $^{11}\text{C}$ ]PIB images, a demonstration was given using two AD images and one typical HC [ $^{11}\text{C}$ ]PIB-RATIO image. The reader was advised to use a rainbow color scale. Subjects with cortical binding (yellow or red) in frontal, cingulate, parietal and temporal cortex were classified as having probable AD, depending on intensity and extent of [ $^{11}\text{C}$ ]PIB uptake.

### ROI analysis

Five neocortical ROIs were considered [33]: the cingulate gyrus, and the frontal, lateral temporal, parietal and occipital cortices. These ROI were defined on individual PET scans using the Hammers maximum probability atlas [34] and SPM5 software (Wellcome Trust Centre for Neuroimaging, UCL, London, UK) as follows. First, T1 MRIs were coregistered to summed activity PIB-PET images without reslicing, then spatially normalized to the MNI/ICBM152 T1 stereotactic template using deformations obtained via Unified Segmentation [35]. The inverse deformation fields were applied to the Hammers atlas to fit the individual T1 anatomy. Probabilistic images of the grey and white matter and CSF tissue classes were obtained in the segmentation step. Gray matter images were thresholded at a probability of  $>0.5$  and multiplied with the atlas resampled in the individual space. Finally, regional activities of the selected ROIs were extracted from 40 to 90 min [ $^{11}\text{C}$ ]PIB RATIO images. Regional values were compared between the three groups using Kruskal-Wallis testing with MedCalc<sup>®</sup>. If significant differences ( $p < 0.05$ ) were observed then intergroup comparisons were performed using Mann-Whitney  $U$  tests.

### Parametric image analysis

Using SPM5, [ $^{11}\text{C}$ ]PIB-RATIO images were spatially normalized to a customized template created from PCA and AD patients' MRIs. Pairwise comparisons were performed between groups (control, PCA and AD), and PCA patients compared individually with the AD group. A voxel based ANCOVA with age as a covariate was used to identify clusters of voxels that significantly differed in these comparisons. Global cerebral mean was used as group specific covariate in a second analysis. Statistical parametric maps resulting from contrasts of comparisons were thresholded at  $p_{\text{uncorr}} < 0.001$  at the voxel level. Further thresholding at  $p_{\text{uncorr}} < 0.001$  at the cluster level, with a minimum cluster extent of 350 voxels, led to a joint probability significance level of  $p_{\text{corr}} < 0.01$  corrected for multiple comparisons at the cluster level.

## Results

### Demographic and clinical data

Simultanagnosia, alexia, acalculia, agraphia, ideomotor and constructional apraxia were the most frequent signs (Table 1). Two patients had a left hemianopia (cases 2 and 5). Mild signs of symmetrical parkinsonism were noticed in two patients (cases 1 and 3). One patient had visual

hallucinations (case 5). None had fluctuation of cognitive or motor symptoms. No patient had more than one of these three cardinal symptoms, and therefore, none fulfilled clinical criteria for dementia with Lewy bodies (DLB). None showed evidence of motor signs such as asymmetrical or unilateral parkinsonism with gestural apraxia or dystonia consistent with corticobasal degeneration (CBD). PCA patients were younger than AD patients ( $p < 0.05$ ). PCA patients' symptoms had been progressing for 1 to 4 years at the clinical evaluation, compared with 1 to 5 years for AD patients (n.s). Level of education was also comparable in the two groups (Table 3). MRI most often showed asymmetrical cortical or subcortical atrophy in the parietal and occipital regions. No PCA patient had medial temporal lobe or hippocampal atrophy suggesting typical AD.

### Neuropsychological deficits

Cognitive functions of PCA patients were variably affected with a mean MMSE ranging from 15 to 28. Impact of cognitive disorders on autonomy was also variable from one subject to another with a CDR ranging from 0.5 to 1 (Table 1). PCA and AD patients were not significantly different in terms of global cognitive function as measured with MMSE and CDR. Visuoceptive, visuospatial and visuoconstructive abilities were systematically affected for the five PCA patients. Their visuoconstructive apraxia as assessed with figure copying was more important than that of AD patients ( $p = 0.008$ ). Verbal memory was preserved in two PCA patients (cases 1 and 2), mildly impaired in one patient (case 5) and moderately altered in two patients (cases 3 and 4). Because of his visual impairment, patient 4 could not perform FCSRT. His memory performance as assessed using the French version of the California Verbal Learning Test was moderately reduced (data not shown). Memory deficits evaluated with the FCSRT in the four other PCA patients was less severe than in AD patients (free delayed recall,  $p = 0.02$ ; total delayed recall,  $p = 0.048$ ). Executive functions were systematically but variably affected. PCA patients were slower than AD patients during the TMT-A ( $p = 0.02$ ). Naming was preserved in two PCA cases (1 and 3) and impaired in the others (Table 3).

### CSF data

Among our five PCA patients (Table 4), three fulfilled biological criteria for typical AD with abnormal levels of the three CSF markers (cases 1, 2 and 5). Two PCA patients were classified as atypical AD due to abnormalities of either tau or amyloid protein levels (cases 3 and 4). None had normal CSF biomarkers. Thus, all of PCA patients showed a biological profile consistent with AD, either typical or atypical.

**Table 4** CSF biomarker profile and PIB-PET pattern of PCA patients

Subjects	Aβ <sub>1-42</sub> (pg/mL)	T-tau (pg/mL)	P-tau181 (pg/mL)	CSF profile	PIB-PET pattern
PCA 1	441	450	69	Typical AD	Probable AD
PCA 2	461	618	107	Typical AD	Probable AD
PCA 3	573	582	107	<i>Atypical AD</i>	Probable AD
PCA 4	216	241	48	<i>Atypical AD</i>	Probable AD
PCA 5	389	1128	143	Typical AD	Probable AD

CSF pattern is considered atypical for patients presenting either elevated T-tau and P-tau181 or decreased Aβ<sub>42</sub> concentrations. Normal levels of T-tau, P-tau181 or Aβ<sub>42</sub> and atypical CSF profile are shown in italics. Subjects are considered to have a typical AD profile if all three levels lay beyond determined CSF cut-off values. PIB-PET pattern is consistent with a probable AD when showing neocortical retention of [<sup>11</sup>C]PIB

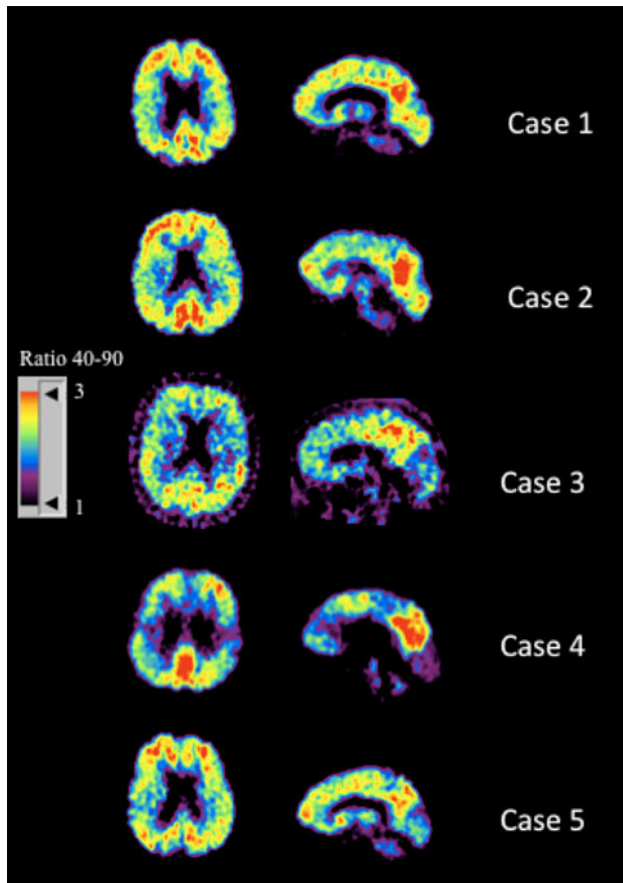


**Fig. 1** [<sup>11</sup>C]PIB-PET images of PCA patients. [<sup>11</sup>C]PIB-RATIO images of all PCA patients show an extensive but variable cortical [<sup>11</sup>C]PIB uptake in frontal, temporal, parietal, occipital and cingulate cortices consistent with amyloid deposition and probable AD. [<sup>11</sup>C]PIB uptake in posterior regions is variable from one PCA subject to another

[<sup>11</sup>C]PIB data

Visual analysis

Visual inspection of the quantitative data showed neocortical retention of [<sup>11</sup>C]PIB in all PCA patients (Table 3), as in AD subjects, suggesting underlying amyloid pathology.

No [<sup>11</sup>C]PIB-RATIO scans of our PCA patients were considered as normal or doubtful (Table 4, Fig. 1).

ROI analysis (Fig. 2)

PCA, AD versus controls. ROI group analysis showed that AD and PCA patients had significantly higher RATIO values than controls in all five neocortical regions investigated ( $p < 0.001$ ). PCA versus AD. There was no statistical difference of [<sup>11</sup>C]PIB uptake in the frontal cortex ( $p = 0.24$ ), parietal cortex ( $p = 0.14$ ) and cingulate cortex ( $p = 0.88$ ) between PCA and AD patients. PCA patients had a significantly higher RATIO of [<sup>11</sup>C]PIB uptake than AD patients in the occipital cortex ( $p = 0.03$ ). A trend for higher binding in PCA was also noticed in the lateral temporal cortex ( $p = 0.05$ ).

Parametric image analysis (Fig. 3)

PCA, AD versus controls. Both PCA and AD patients had significantly higher [<sup>11</sup>C]PIB uptake in neocortical brain regions than control subjects (data not shown). PCA versus AD. When global mean was not included as a covariate in the analysis, PCA subjects showed a focally higher [<sup>11</sup>C]PIB uptake in the visual cortex, the bilateral occipito-temporal junction, the left parietal cortex and the right temporal cortex, and to a lesser degree in the frontal cortex (Fig. 3, no global). These differences were no longer significant when global cerebral mean was included as a covariate (Fig. 3, global). AD versus PCA. There were no regions of higher [<sup>11</sup>C]PIB RATIO in AD than in PCA patients. Individual comparison of PCA patients with the AD patient group revealed a great heterogeneity of [<sup>11</sup>C]PIB-RATIO patterns. In four PCA patients (cases 1, 2, 3 and 5), the posterior regions showed a significantly higher [<sup>11</sup>C]PIB-RATIO retention than in the AD group. Retention of [<sup>11</sup>C]PIB could encompass the visual cortex on both sides (case 1 and 2), with more variable extension to temporal and parietal cortices (cases 2, 3 and 5). However, two of the four PCA patients (cases 1 and 5) also

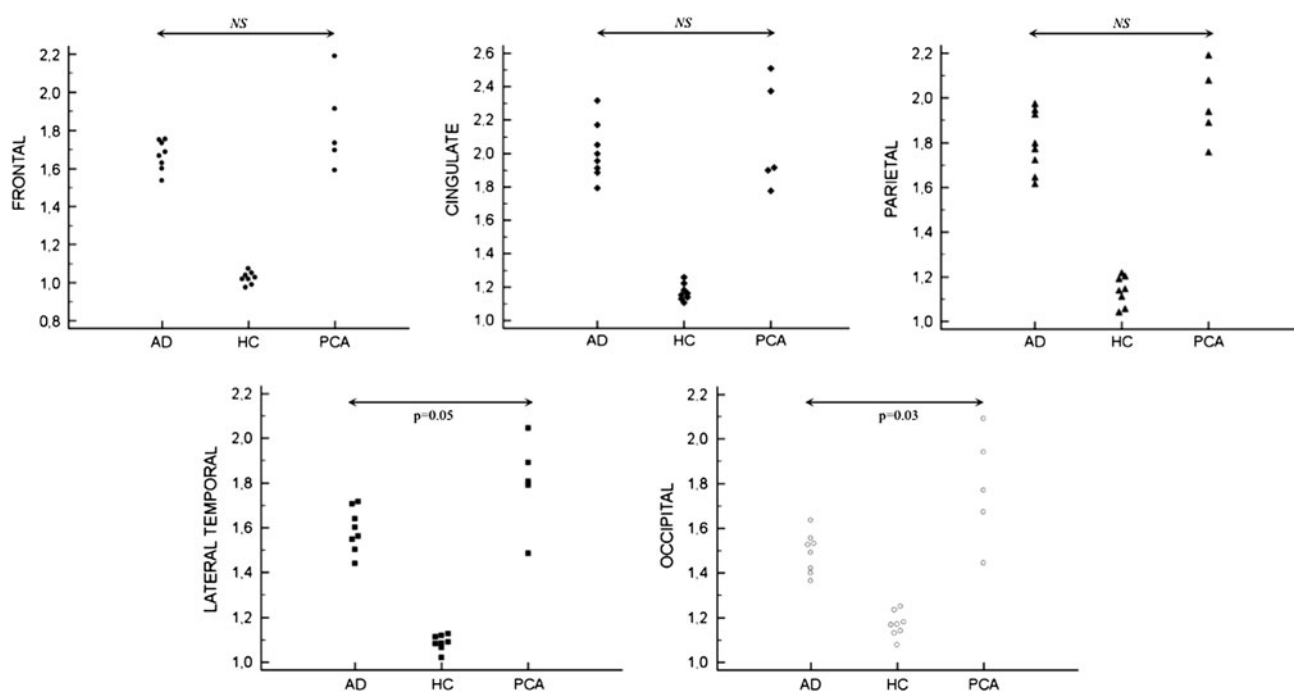


**Fig. 2** ROI analysis of PCA group versus typical AD group. AD and PCA patients have significantly higher RATIO values than controls in all five investigated neocortical regions ( $p < 0.001$ ). There is no statistical difference of [ $^{11}\text{C}$ ]PIB retention in the frontal ( $p = 0.24$ ),

parietal ( $p = 0.14$ ) and cingulate cortices ( $p = 0.88$ ) between PCA and AD patients. PCA patients have a significantly higher RATIO of [ $^{11}\text{C}$ ]PIB uptake than AD in the occipital cortex ( $p = 0.03$ ). A trend is also noticed in lateral temporal cortex ( $p = 0.05$ )

showed a higher [ $^{11}\text{C}$ ]PIB retention in the frontal cortex. Finally, one PCA patient (case 4) did not show higher [ $^{11}\text{C}$ ]PIB retention in any region as compared to the AD group, i.e. his [ $^{11}\text{C}$ ]PIB-RATIO pattern was similar to that of typical AD subjects (Fig. 3).

## Discussion

In this study, the combination of CSF biomarker analysis and [ $^{11}\text{C}$ ]PIB PET scanning in five consecutive prototypical PCA patients demonstrated in vivo a profile overall suggestive of AD both for CSF biomarkers and cerebral amyloid imaging. A posterior cortical distribution of [ $^{11}\text{C}$ ]PIB involving parietal, temporal and occipital cortices, particularly visual cortex, was inconsistently found in individual PCA cases, as well as in the group analyses, but was not significant when global means were taken into account. Our imaging and CSF data suggestive of AD diagnosis are concordant with neuropathological studies showing AD pathology in most PCA cases [2, 3, 9]. There are few studies comparing CSF and PIB results in AD and we found only a single PCA case report in the literature where both biomarkers were available, results of which were consistent with our findings [36]. Our combined biomarker study reinforces the hypothesis that the PCA syndrome is most often a focal form of AD.

Only four case reports, including a total of six patients, have been published to date. They have shown abnormal [ $^{11}\text{C}$ ]PIB retention in PCA using visual inspection [36, 37], ROI analysis [38], or SPM analysis [39], but none combined these three types of analysis.

In our study, SPM and ROI group comparisons showed higher [ $^{11}\text{C}$ ]PIB retention in PCA patients compared with AD patients, with a posterior emphasis (Figs. 2, 3). Visual inspection of scans showed that the five PCA patients had abnormal cortical retention of [ $^{11}\text{C}$ ]PIB of similar magnitude as patients with typical AD (Fig. 1). However, individual SPM analyses showed a pattern of cortical [ $^{11}\text{C}$ ]PIB retention that significantly differed from the AD group, with higher amyloid burden in the primary visual cortex, in the parietal or the temporal cortices. Two patients also had a higher [ $^{11}\text{C}$ ]PIB uptake in anterior regions. Only one PCA patient had a pattern not distinguishable from AD, i.e. 4/5 did show differences, indicating that such analyses may be clinically relevant.

ROI and SPM individual analyses also showed a great interregional variability in [ $^{11}\text{C}$ ]PIB uptake in patients compared to control subjects, particularly for the PCA group (Figs. 2, 3). The posterior-anterior gradient of amyloid load seen in a majority of our PCA patients may be related to a particular distribution pattern of lesions as shown in autopsied cases [2, 10]. Indeed, these authors found more numerous SPs in occipital [2] or occipito-



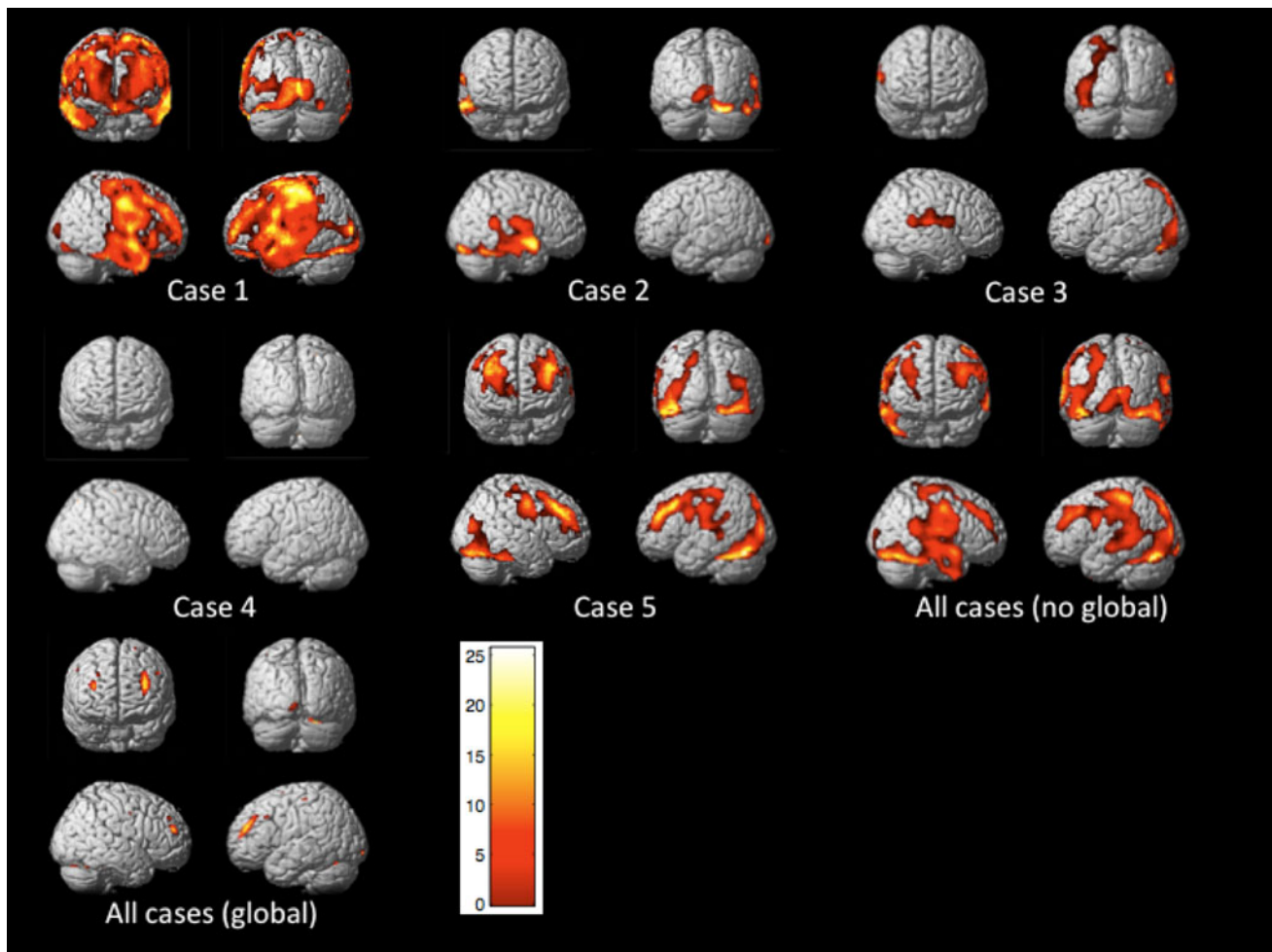


**Fig. 3** SPM analysis of individual PCA patients and PCA group vs typical AD group. Individual analysis. Four PCA patients (cases 1, 2, 3 and 5) show a significantly higher retention of [ $^{11}\text{C}$ ]PIB than typical AD in posterior regions with a variable pattern including occipital, temporal and/or parietal cortices. Two of these four PCA patients (cases 1 and 5) also show a higher [ $^{11}\text{C}$ ]PIB retention in the anterior regions. One case (case 4) presents a [ $^{11}\text{C}$ ]PIB uptake pattern similar

parietal regions [10] than in frontal regions [10] and hippocampus [2]. However, these data seem less robust than those related to NFTs, showing higher density in posterior regions in PCA compared to AD. Thus, the pattern of posterior predominance of PIB uptake was no longer found when the overall level of PIB binding was included as a covariate in the SPM group comparison (Fig. 3). This discrepancy is likely to be due to a global higher [ $^{11}\text{C}$ ]PIB retention in PCA compared to AD (Fig. 2).

Some previous PIB-PET studies showed a positive correlation between [ $^{11}\text{C}$ ]PIB uptake, severity of cognitive deficit in AD [40], hypometabolism [41] and level of education [42]. These variables, as well as disease duration, were, however, not different between groups in our sample, and hence do not explain the higher amyloid load in our PCA group. Age is unlikely to underlie the global

difference, even if the patients in the PCA group were younger, this variable having been included as a covariate in the SPM analysis. In the same way, another study did not show any correlation between [ $^{11}\text{C}$ ]PIB uptake and age at onset, clinical status or glucose metabolism in AD [43]. Higher NFT density and more severe neuronal loss were shown in early-onset PCA compared to late-onset cases [10] whereas differences in amyloid load were not reported.

Increased [ $^{11}\text{C}$ ]PIB retention in neocortical regions in our AD group compared to controls is consistent with the literature [14, 15, 42, 44]. The five PCA patients had neocortical [ $^{11}\text{C}$ ]PIB retention comparable to AD patients. PIB positivity is highly suggestive of amyloid deposition [16]. It correlates with the presence and the concentration of neuritic plaques characteristic of AD [18]. It is indicative

to that of typical AD subjects. Group analysis. When global mean is not included as a covariate in the analysis, PCA subjects, in comparison to AD patients, show a focally higher [ $^{11}\text{C}$ ]PIB retention in the visual cortex, the bilateral occipito-temporal junction, the left parietal and the right temporal cortices but also in frontal cortex at a lesser degree. These differences are no longer found with global cerebral mean as a covariate

of amyloid brain pathology, but not pathognomonic of AD. Amyloid deposits can also be found in DLB [45, 46], and in non-demented aged controls [47, 48]. Based on [ $^{11}\text{C}$ ]PIB data, our five PCA patients have increased amyloid concentrations and are likely to have AD pathology. None of them have symptoms consistent with DLB or CBD, which is also in line with this hypothesis.

CSF showed decreased  $A\beta_{42}$  levels in four patients and elevated levels of T-tau and P-tau181 in a partially overlapping group of four others. According to our results, three of the five PCA patients (cases 1, 2 and 5) showed a typical AD CSF profile. The two others (cases 3 and 4) with either elevated CSF tau or decreased  $A\beta_{42}$  showed a less typical profile, which is nevertheless consistent with AD. Our study thus identified a dominant AD type biological profile in PCA. These findings are in accordance with published studies with CSF analysis in PCA [49] (Seguin et al., in press). Decreased CSF  $A\beta_{42}$  and elevated phosphorylated tau at threonine 199 levels have been reported in a single case of PCA [36].

Decreased levels of CSF  $A\beta_{42}$ , which have been linked to trapping of the protein in senile plaques [50], is a reliable marker of AD pathology, with a variable diagnostic sensitivity (58–96%) and specificity (61–86%). Taking into account increased levels of T-tau protein and P-tau181 protein also helps to identify AD patients with a sensitivity of 65–80% and specificity of 60–92% in different studies with post-mortem confirmation of diagnosis [12, 51, 52]. Combining the three biomarkers achieves sensitivities and specificities of about 90% [30, 53]. Cut-off values used in our study are compatible with normative data of most laboratories [30–32, 54], and we are confident in the AD diagnosis of our patients with typical AD CSF profiles.

Atypical CSF patterns have previously been described in patients with autopsy-based diagnosis of AD [55] and remain consistent with underlying AD pathology. However, these CSF profiles are less specific of AD and can be found in other neurodegenerative diseases, sometimes associated with AD. CSF profiles with low  $A\beta_{42}$  and normal tau proteins level have been found in particular in patients showing AD lesions in association with DLB [56], vascular dementia, or Parkinson's disease with dementia [55]. Similarly, CSF profiles with normal  $A\beta_{42}$  and elevated tau and P-tau181 levels were described in autopsied cases, either with vascular dementia or DLB [55]. None of our patients, even those with atypical CSF patterns, fulfilled diagnostic criteria for DLB. They are therefore most likely to have underlying AD, but DLB associated with AD pathology remains a differential diagnosis.

Although histological data were not available and the sample size was small, our results indicated that a combination of biomarkers could demonstrate amyloid burden in vivo in PCA, suggesting a diagnosis of AD in these

patients. We could not formally exclude associated DLB pathology, but our PET and CSF data were consistent with those of neuropathological studies in PCA. Our results also showed a posterior regional pattern of amyloid deposits in PCA. Although this finding was reminiscent of the regional distribution of histological lesions, it was partially explained by a globally higher [ $^{11}\text{C}$ ]PIB retention in PCA as compared to AD in our sample. This higher amyloid burden in PCA compared to AD was not related to age at onset, disease severity, disease duration or level of education.

Although post mortem examination remains the only way to determine the whole spectrum of pathological events related to this clinical condition, we found combined CSF and PET biomarkers helpful in the in vivo diagnosis of PCA with underlying AD pathology.

**Conflict of interest** None.

## References

- Benson DF, Davis RJ, Snyder BD (1988) Posterior cortical atrophy. *Arch Neurol* 45(7):789–793
- Tang-Wai DF et al (2004) Clinical, genetic, and neuropathologic characteristics of posterior cortical atrophy. *Neurology* 63(7):1168–1174
- Renner JA et al (2004) Progressive posterior cortical dysfunction: a clinicopathologic series. *Neurology* 63(7):1175–1180
- McMonagle P et al (2006) The cognitive profile of posterior cortical atrophy. *Neurology* 66(3):331–338
- Formaglio M et al (2009) Homonymous hemianopia and posterior cortical atrophy. *Rev Neurol (Paris)* 165(3):256–62
- Whitwell JL et al (2007) Imaging correlates of posterior cortical atrophy. *Neurobiol Aging* 28(7):1051–1061
- Nestor PJ et al (2003) The topography of metabolic deficits in posterior cortical atrophy (the visual variant of Alzheimer's disease) with FDG-PET. *J Neurol Neurosurg Psychiatry* 74(11):1521–1529
- Schmidtke K, Hull M, Talazko J (2005) Posterior cortical atrophy: variant of Alzheimer's disease? A case series with PET findings. *J Neurol* 252(1):27–35
- Alladi S et al (2007) Focal cortical presentations of Alzheimer's disease. *Brain* 130(Pt 10):2636–2645
- Hof PR et al (1997) Atypical form of Alzheimer's disease with prominent posterior cortical atrophy: a review of lesion distribution and circuit disconnection in cortical visual pathways. *Vision Res* 37(24):3609–3625
- Hulstaert F et al (1999) Improved discrimination of AD patients using beta-amyloid(1–42) and tau levels in CSF. *Neurology* 52(8):1555–1562
- Shaw LM et al (2009) Cerebrospinal fluid biomarker signature in Alzheimer's disease neuroimaging initiative subjects. *Ann Neurol* 65(4):403–413
- Mathis CA et al (2002) A lipophilic thioflavin-T derivative for positron emission tomography (PET) imaging of amyloid in brain. *Bioorg Med Chem Lett* 12(3):295–298
- Klunk WE et al (2004) Imaging brain amyloid in Alzheimer's disease with Pittsburgh Compound-B. *Ann Neurol* 55(3):306–319
- Engler H et al (2006) Two-year follow-up of amyloid deposition in patients with Alzheimer's disease. *Brain* 129(Pt 11):2856–2866

16. Bacskai BJ et al (2007) Molecular imaging with Pittsburgh Compound B confirmed at autopsy: a case report. *Arch Neurol* 64(3):431–434
17. Lockhart A et al (2007) PIB is a non-specific imaging marker of amyloid-beta (Abeta) peptide-related cerebral amyloidosis. *Brain* 130(Pt 10):2607–2615
18. Ikonomic MD et al (2008) Post-mortem correlates of in vivo PiB-PET amyloid imaging in a typical case of Alzheimer's disease. *Brain* 131(Pt 6):1630–1645
19. Folstein MFFS, McHugh PR (1975) Mini-mental state. A practical method for grading the cognitive state of patients for the clinician. *J Psychiatr Res* 12:189–198
20. Morris JC (1993) The clinical dementia rating (CDR): current version and scoring rules. *Neurology* 43(11):2412–2414
21. McKhann G et al (1984) Clinical diagnosis of Alzheimer's disease: report of the NINCDS-ADRDA Work Group under the auspices of Department of Health and Human Services Task Force on Alzheimer's disease. *Neurology* 34(7):939–944
22. Grober E, Buschke H (1987) Genuine memory deficits in dementia. *Dev Psychol* 3:13–36
23. Delis D et al (1987) The California Verbal Learning Test (research Edition). Psychological corporation, New York
24. Cardebat DDB, Puel M, Goulet P, Joanne Y (1990) Formal and semantic lexical evocation in normal subjects. Performance and dynamics of production as a function of sex, age and educational level. *Acta Neurol Belg* 90:207–217
25. Bachy-Langedock N (1989) Batterie d'examen des troubles en denomination, Editest, Bruxelles
26. Stroop (1935) Studies of interferences in serial verbal reactions. *J Exp Psychol* 18:643–662
27. Reitan RM, Wolfson D (2004) The Trail Making Test as an initial screening procedure for neuropsychological impairment in older children. *Arch Clin Neuropsychol* 19(2):281–288
28. Rapport LJ, Millis SR, Bonello PJ (1998) Validation of the Warrington theory of visual processing and the visual object and space perception battery. *J Clin Exp Neuropsychol* 20(2):211–220
29. Sunderland T et al (1989) Clock drawing in Alzheimer's disease. A novel measure of dementia severity. *J Am Geriatr Soc* 37(8):725–729
30. Hansson O et al (2006) Association between CSF biomarkers and incipient Alzheimer's disease in patients with mild cognitive impairment: a follow-up study. *Lancet Neurol* 5(3):228–234
31. Tapiola T et al (2009) Cerebrospinal fluid {beta}-amyloid 42 and tau proteins as biomarkers of Alzheimer-type pathologic changes in the brain. *Arch Neurol* 66(3):382–389
32. Mattsson N et al (2009) CSF biomarkers and incipient Alzheimer disease in patients with mild cognitive impairment. *Jama* 302(4):385–393
33. Lopresti BJ et al (2005) Simplified quantification of Pittsburgh Compound B amyloid imaging PET studies: a comparative analysis. *J Nucl Med* 46(12):1959–1972
34. Hammers A et al (2003) Three-dimensional maximum probability atlas of the human brain, with particular reference to the temporal lobe. *Hum Brain Mapp* 19(4):224–247
35. Ashburner J, Friston KJ (2005) Unified segmentation. *Neuroimage* 26(3):839–851
36. Kambe T et al (2010) Posterior cortical atrophy with [11C] Pittsburgh compound B accumulation in the primary visual cortex. *J Neurol* 257(3):469–471
37. Migliaccio R et al (2009) Clinical syndromes associated with posterior atrophy: early age at onset AD spectrum. *Neurology* 73(19):1571–1578
38. Tenovuo O et al (2008) Posterior cortical atrophy: a rare form of dementia with in vivo evidence of amyloid-beta accumulation. *J Alzheimers Dis* 15(3):351–355
39. Ng SY et al (2007) Evaluating atypical dementia syndromes using positron emission tomography with carbon 11 labeled Pittsburgh Compound B. *Arch Neurol* 64(8):1140–1144
40. Grimmer T et al (2009) Clinical severity of Alzheimer's disease is associated with PIB uptake in PET. *Neurobiol Aging* 30(12):1902–1909
41. Edison P et al (2007) Amyloid, hypometabolism, and cognition in Alzheimer disease: an [11C]PIB and [18F]FDG PET study. *Neurology* 68(7):501–508
42. Kempainen NM et al (2007) PET amyloid ligand [11C]PIB uptake is increased in mild cognitive impairment. *Neurology* 68(19):1603–1606
43. Rabinovici GD et al (2010) Increased metabolic vulnerability in early-onset Alzheimer's disease is not related to amyloid burden. *Brain* 133(Pt 2): p 512–28
44. Forsberg A et al (2008) PET imaging of amyloid deposition in patients with mild cognitive impairment. *Neurobiol Aging* 29(10):1456–1465
45. Gomperts SN et al (2008) Imaging amyloid deposition in Lewy body diseases. *Neurology* 71(12):903–910
46. Edison P et al (2008) Amyloid load in Parkinson's disease dementia and Lewy body dementia measured with [11C]PIB positron emission tomography. *J Neurol Neurosurg Psychiatry* 79(12):1331–1338
47. Pike KE et al (2007) Beta-amyloid imaging and memory in non-demented individuals: evidence for preclinical Alzheimer's disease. *Brain* 130(Pt 11):2837–2844
48. Villemagne VL et al (2008) Abeta deposits in older non-demented individuals with cognitive decline are indicative of preclinical Alzheimer's disease. *Neuropsychologia* 46(6):1688–1697
49. Baumann TP et al (2010) CSF-Tau and CSF-Abeta(1–42) in posterior cortical atrophy. *Dement Geriatr Cogn Disord* 29(6):530–533
50. Strozzyk D et al (2003) CSF Abeta 42 levels correlate with amyloid-neuropathology in a population-based autopsy study. *Neurology* 60(4):652–656
51. Roher AE et al (2009) Proteomics-derived cerebrospinal fluid markers of autopsy-confirmed Alzheimer's disease. *Biomarkers* 14(7):493–501
52. Koopman K et al (2009) Improved discrimination of autopsy-confirmed Alzheimer's disease (AD) from non-AD dementias using CSF P-tau(181P). *Neurochem Int* 55(4):214–218
53. Mulder C et al (2010) Amyloid-beta(1-42), total tau, and phosphorylated tau as cerebrospinal fluid biomarkers for the diagnosis of Alzheimer disease. *Clin Chem* 56(2):248–53
54. Hort J et al (2010) Use of cerebrospinal fluid biomarkers in diagnosis of dementia across Europe. *Eur J Neurol* 17(1):90–6
55. Engelborghs S et al (2008) Diagnostic performance of a CSF-biomarker panel in autopsy-confirmed dementia. *Neurobiol Aging* 29(8):1143–1159
56. Iqbal K et al (2005) Subgroups of Alzheimer's disease based on cerebrospinal fluid molecular markers. *Ann Neurol* 58(5):748–757